Autonomous Induction Generator/Rectifier as Regulated DC Power Supply for Hybrid Renewable Energy Systems

Ali Nesba, Rachid Ibtiouen, Said Mektouib, Omar Touhami, Noureddine Takorabet

7th WSEAS Int. Conf. on MATHEMATICAL METHODS and COMPUTATIONAL TECHNIQUES IN ELECTRICAL ENGINEERING, Sofia, 27-29/10/05 (pp162-167)

Autonomous Induction Generator/Rectifier as Regulated DC Power Supply for Hybrid Renewable Energy Systems

A. NESBA[1], R. IBTIOUEN[1], S. MEKHTOUB[1], O. TOUHAMI[1] and N. TAKORABET[2]

[1]Department of Electrical Engineering
National Polytechnic School
BP 182 El-Harrach 16200 Algiers Algeria
ALGERIA
Rachid.ibtiouen@enp.edu.dz http://www.enp.edu.dz

[2]Groupe de Recherche en Électrotechnique et Électronique de Nancy - ENSEM
Institut National Polytechnique de Lorraine
2 av. de la Forêt de Haye 54516 Vandoeuvre Nancy Cedex
FRANCE
http://www.ensem.inpl-nancy.fr/rgreen/rgreen.php

Abstract: - The present article deals with the wind power-generating unit of a Hybrid Photovoltaic – Wind Renewable Energy System (HPVWRES). The dynamic flux model of the self-excited induction generator used in the wind power-generating unit is given. This model, known to account for magnetic saturation is validated by experimental results. Operations under variable wind speed and/or variable load are discussed.

Key-Words: - Hybrid, Induction Generator, Modeling, Rectifier, Regulation, Renewable Energy, Experimental investigation.

1 Introduction

The increasing global need for energy, environmental concerns and the high cost of delivering power to remote areas in many developing countries, together with the recent renewed interest in renewable energy and the steady progress in power electronics, constitute strong motivations for carrying investigations in the field of renewable energy systems[1]-[3]. Photovoltaic (PV) and wind generators are particularly widely used components in such systems.

The present article deals with a hybrid PV-Wind renewable energy system (HPVWRES) and only the wind power-generating unit is considered in this part of the work. The PV generators provide power under DC voltage. The DC/DC converter (Figure 1) is a peak-power tracker used in optimizing the efficiency of the PV generators. The wind generator produces power under AC voltage, which is converted into a constant DC voltage by the controlled AC/DC converter. The HPVWRES uses storage batteries to produce power during periods of time in which wind speed and insolation level become insufficient. Power delivered by the AC/DC, DC/DC converters and/or the storage batteries is used directly under DC voltage and/or AC voltage via an inverter. The control unit

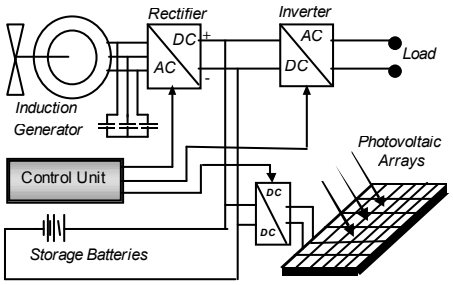

Fig. 1. Hybrid PV-Wind renewable energy system.

ensures the monitoring of the HPVWRES components and parameters (converters, wind speed, insolation…).

The present paper studies the wind power generation in the HPVWRES made up of a three-phase induction generator, a bank of excitation capacitors and a controlled AC/DC converter (Figure 2). The second and third sections of this paper describe the models of the induction generator and AC/DC converter. Section four examines the performance of the wind power-generating unit (WPGU). Computed results are presented. Operations under (i) constant load and variable wind speed, (ii) variable load and constant wind speed are discussed.

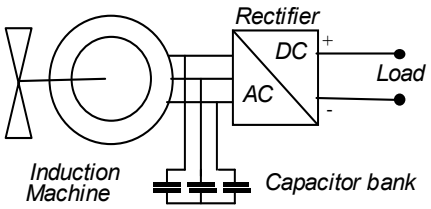

Fig. 2. Wind power generating unit

2 Induction Generator

The generator used by the WPGU is a three-phase self-excited induction generator (SEIG). In fact, in recent years, self-excited induction generators have been widely used as suitable power sources, particularly in renewable power generating systems such as in hydroelectric and wind energy applications [4]-[8]. Robust and brushless construction (squirrel-cage rotor), low maintenance requirements, absence of DC power supply for field excitation, small seize, reduced cost, better transient performance, self-protection against short-circuits and large over loads, are some of the advantages of the induction generator over the synchronous and DC generators. The induction generator self-excitation phenomenon is known as early as the beginning of the twentieth century [9]. It was demonstrated then that an externally driven induction machine can operate as a generator if a reactive power source is available to provide excitation for the machine. The self-excitation can be achieved when a capacitor bank with an appropriate value is properly connected across the machine terminals.

Here a dynamic flux model for the SEIG that accounts for magnetic saturation is developed and validated by experimental results. These results describe the stator voltage of the SEIG during the self-excitation process and during sudden connection of the load onto the machine terminals.

2.1 Induction Machine Flux Model

The equations for the induction machine voltage in the q-d axis arbitrary reference frame may be expressed as [10]-[12]:

$$v_{qs} = r_s i_{qs} + \omega \varphi_{ds} + p \varphi_{qs} \quad (1)$$

$$v_{ds} = r_s i_{ds} - \omega \varphi_{qs} + p \varphi_{ds} \quad (2)$$

$$v'_{qr} = r'_r i'_{qr} + (\omega - \omega_r) \varphi'_{dr} + p \varphi'_{qr} \quad (3)$$

$$v'_{dr} = r'_r i'_{dr} - (\omega - \omega_r) \varphi'_{qr} + p \varphi'_{dr} \quad (4)$$

Note that in the above relations, all rotor quantities and parameters refer to the stator. p = d/dt denotes the differential operator with respect to time t. ω and ω_r are the angular speeds of the reference frame and the rotor respectively. v_{qs} , v_{ds} , v'_{qr} and v'_{dr} denote the q-d axis components of the stator and rotor voltages (with respect to the stator) respectively. i_{qs}, i_{ds}, i'_{qr}, i'_{dr}, represent the q-d axis components of the stator and rotor currents (with respect to the stator) respectively. φ_{qs} , φ_{ds} , φ'_{qr} and φ'_{dr} represent the q-d axis components of the stator, and rotor fluxes (with respect to the stator) respectively. Finally, r_s and r'_r denote stator and rotor resistances (with respect to the stator).

The stator and rotor currents, in terms of q-d axis fluxes can be written as:

$$i_{qs} = \frac{\varphi_{qs} - \varphi_{mq}}{l_s} \quad (5)$$

$$i_{ds} = \frac{\varphi_{ds} - \varphi_{md}}{l_s} \quad (6)$$

$$i'_{qr} = \frac{\varphi'_{qr} - \varphi_{mq}}{l'_r} \quad (7)$$

$$i'_{dr} = \frac{\varphi'_{dr} - \varphi_{md}}{l'_r} \quad (8)$$

where l_s and l'_r denote stator and rotor leakage inductances referred to the stator. φ_{mq} and φ_{md} denote the q-d axis components of the magnetizing flux. They are useful quantities when it comes to represent saturation and are defined by:

$$\varphi_{mq} = M(i_{qs} + i'_{qr}) \quad (9)$$

$$\varphi_{md} = M(i_{ds} + i'_{dr}) \quad (10)$$

$$M = \frac{3}{2} L_{ms} \quad (11)$$

an expression in which L_{ms} represents the stator magnetizing inductance.

The use of (5)-(8) helps eliminate the currents in (9) and (10) as well as in the voltage equations given by (1)-(4), and if the resulting voltage equations are solved for the q-d axis fluxes, the following state equations can be obtained:

$$p\varphi_{qs} = v_{qs} - \omega\varphi_{ds} + \frac{r_s}{l_s}(\varphi_{mq} - \varphi_{qs}) \quad (12)$$

$$p\varphi_{ds} = v_{ds} + \omega\varphi_{qs} + \frac{r_s}{l_s}(\varphi_{md} - \varphi_{ds}) \quad (13)$$

$$p\varphi_{q'r} = v_{q'r} - (\omega - \omega_r)\varphi_{d'r} + \frac{r_{r'}}{l_{r'}}(\varphi_{mq} - \varphi_{q'r}) \quad (14)$$

$$p\varphi_{d'r} = v_{d'r} + (\omega - \omega_r)\varphi_{q'r} + \frac{r_{r'}}{l_{r'}}(\varphi_{md} - \varphi_{d'r}) \quad (15)$$

For a self-excited induction generator, the voltage-current equations of the excitation capacitor are expressed in the arbitrary reference frame as:

$$p\, v_{qs} = \frac{1}{C_e} i_{qs} - \omega\, v_{ds} \quad (16)$$

$$p\, v_{ds} = \frac{1}{C_e} i_{ds} - \omega\, v_{qs} \quad (17)$$

Here C_e denotes the excitation capacitance.

If the studied induction generator is assumed to be magnetically linear, the SEIG flux model, in the arbitrary reference frame, may be obtained by the use of the magnetizing flux expressions (9) and (10), the set of conventional state equations (12)-(15) and the self-excitation equations (16)-(17).

However, the modeling of the SEIG under the assumption of magnetic linearity leads to unrealistic results. The following section presents briefly the method used in this paper which takes account of the saturation effect.

2.2 Saturation Model

The saturation effect in the main flux path of the induction machine is accounted in the framework of an accurate technique that makes use of an analytical model for the magnetizing inductance M. A combination of exponential, polynomial and arctangent functions is used in this model in order to maximize accuracy. A least-square optimization method is applied for the determination of the model coefficients.

This model writes as follows:

$$M=\begin{cases} M_l & if\ I_m \le I_0 \\ M_s & if\ I_m > I_0 \end{cases} \qquad (18)$$

Where M_l is the value of the magnetizing inductance of the machine in the linear region and M_s its expression in the saturated region. I_m denotes the rms magnetizing current and I_0 is the value of I_m at the upper limit of the linear region.

The expression of M_s is given by

$$M_s = C_1\, atan(C_2(I_m - I_0)) + \cdots$$
$$\cdots + C_3(1-exp(-(I_m-I_0))) + C_4(I_m-I_0) + C_5 \qquad (19)$$

The coefficients C_i, I_0 and M_l are identified using a least-square optimization method. The relative difference between test data and the model for M is within 1e-6. Model-based computed values and measured values of the magnetizing inductance as a function of the magnetizing current are shown in the Figure 3.

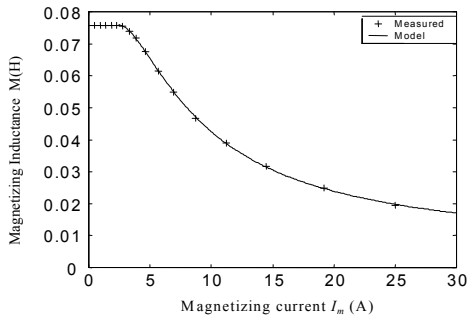

Fig. 3. Variation of the saturated magnetization inductance of the studied machine versus the magnetization current.

The introduction of the main flux saturation effect into the dynamic flux model of the induction machine is essentially based on the knowledge of the q and d magnetizing flux components φ_{mq} and φ_{md}. These components may be expressed as follows:

$$\varphi_{mq} = L_q\left(\frac{\varphi_{qs}}{l_s} + \frac{\varphi'_{qr}}{l'_r}\right) \qquad (20)$$

$$\varphi_{md} = L_d\left(\frac{\varphi_{ds}}{l_s} + \frac{\varphi'_{dr}}{l'_r}\right) \qquad (21)$$

where we have:

$$L_q = L_d = \left(\frac{1}{M} + \frac{1}{l_s} + \frac{1}{l'_r}\right)^{-1} \qquad (22)$$

Obviously, L_q, L_d, and consequently φ_{mq} and φ_{md}, are related to the magnetizing inductance M which is a function of the rms magnetizing current (18)-(19). This current is given by:

$$I_m = \sqrt{(i_{mq}^2 + i_{md}^2)/2} \qquad (23)$$

where we have:

$$i_{mq} = i_{qs} + i'_{qr} \qquad (24)$$

$$i_{md} = i_{ds} + i'_{dr} \qquad (25)$$

Finally, the saturated flux model of SEIG in the arbitrary reference frame is obtained by adding the expressions of the magnetizing inductance, fluxes and currents (18)-(25) to the equations of the linear model presented in the previous section.

The results presented below (figures 4-7) describe the stator voltage of the SEIG during the self-excitation process and during sudden connection of the load onto the machine terminals.

It is clear from these results that there is very good agreement between experimentation and simulation and this confirms the validity of the developed model.

Furthermore, it can be seen on figures 6 and 7 above and on Figure 8 below that the voltage produced by the SEIG is highly affected by the connection of the load onto its terminals.

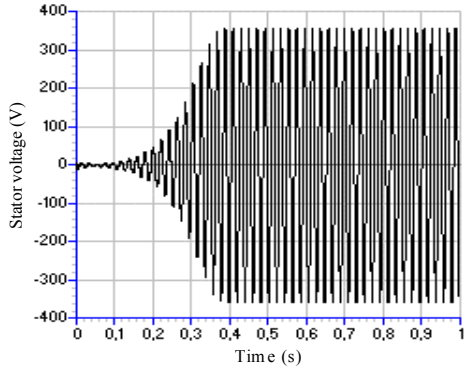

Fig. 4. Computed stator voltage during the self-excitation process at 1500rpm and 90μF.

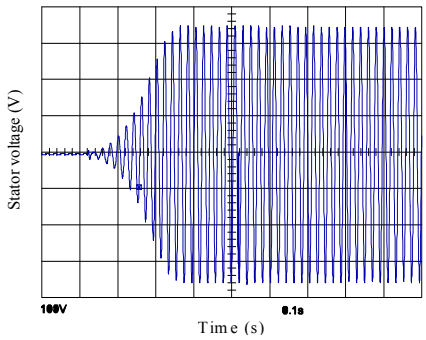

Fig. 5. Measured stator voltage during the self-excitation process at 1500rpm and 90μF.

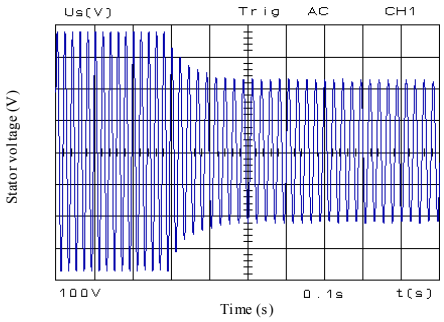

Fig. 6. Measured stator voltage during the connection of the load.

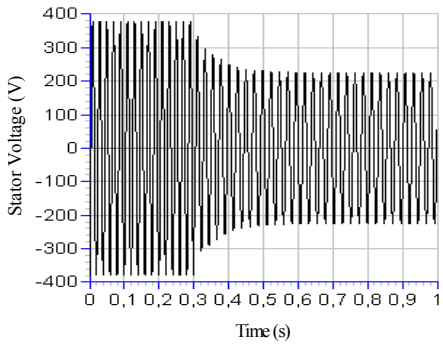

Fig. 7. Computed stator voltage during the connection of the load.

This poor voltage characteristic of the SEIG, especially when feeding an inductive load, constitutes the main disadvantage of this generator and can be referred to the underexcitation of the machine. In fact, the connection of the load, causes the reactive power absorbed by the load and by the leakage reactance of the generator to increase. On the other hand, it engenders some voltage drop in the stator windings, which consequently causes the voltage across the excitation capacitors to decrease, and, as a result, the reactive power produced by these capacitors to also decrease. This diminution in the reactive power produced by the SEIG (capacitors), in addition to the increase of the demand of reactive power (load), constrain the SEIG to operate with weak excitation and thus, with lower output voltage.

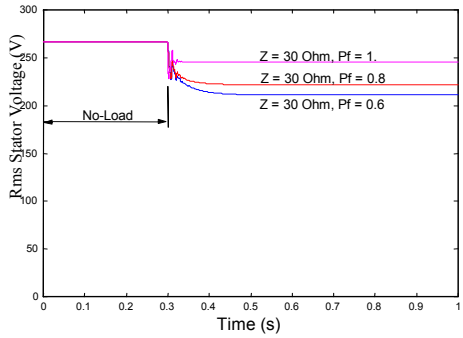

Fig. 8. Computed rms stator voltage during the connection of the load.

The perturbation provoked by the connection of an inductive load on the rms stator voltage is shown by the figure 8. Cases of 0.8 and 0.6 (lagging) power factor are presented. In both cases the load has the same impedance (Z=15Ω). Cases of 0.8 and 0.6 lagging power factor are also compared with the case of unit power factor (Figure 8).

It will also be seen later that the SEIG stator voltage is likewise affected by the rotor speed. The WPGU that we are proposing in this paper remedies to these disadvantages of the SEIG by using a controlled AD/DC converter. This converter produces a constant DC voltage that can be used as it is or be converted to a constant AC voltage by means of a DC/AC converter.

3 Controlled Converter

The converter used in the WPGU is a three-phase AC/DC controlled thyristors converter (Figure 9). This converter uses the SEIG output AC voltage to generate a constant DC voltage. An automatic control ensured by an appropriate controller that operates on the firing angle of the thyristors maintains a constant DC output voltage for a wide variation of the frequency and magnitude of the SEIG stator voltage.

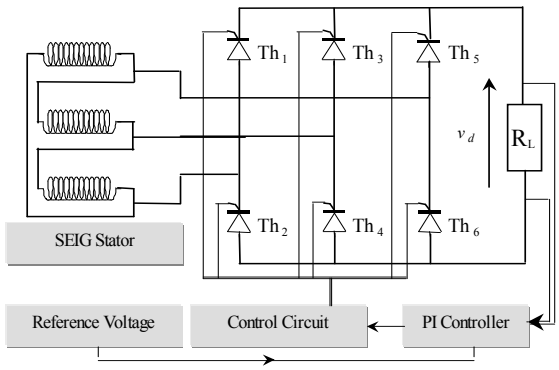

Fig. 9. The AC/DC controlled converter.

4 Experimental Verification

In this section, experimental tests of the WPGU are presented (Figure 10). These results show the effect of the variation of the SEIG rotor speed and load resistance on the output voltage of the WPGU.

A laboratory prototype of a three-phase semi-bridge converter is used. This one-quadrant converter uses three diodes and only three thyristors. It is, therefore, more adequate for the WPGU which requires no inversion capability, it is also more economical than the bridge converter.

Although the output voltage of the SEIG is considerably affected by the variation of the rotor speed, the average value of the DC output voltage of the WPGU, is maintained constant. This fact may clearly be seen on the figure 10, where the measured voltage at the output of the WPGU is shown along with its filtered curve. A 2nd-order Butterworth low pass filter was used to obtain the filtered curve. It is also represented on the figure 10, the reference voltage (200V).

It is obvious that the WPGU produces a constant DC output voltage even though the AC output voltage of the SEIG is significantly influenced by the rotor speed.

Figure 11 shows the effect of the variation of the load on the output voltages of the SEIG and of the whole WPGU.

Although the output voltage of the SEIG is significantly influenced by the variation of the load (voltage rise of approximately 28 %), the average value of the DC output voltage of the WPGU, remains unaltered.

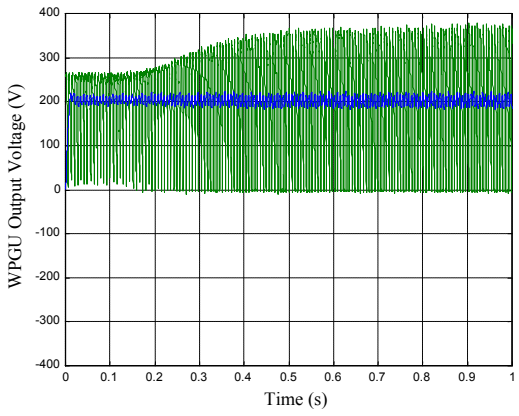

Fig. 10. The WPGU output voltage, filtered and reference voltage when the rotor speed is increased from 1400rpm up to 1600rpm (measured).

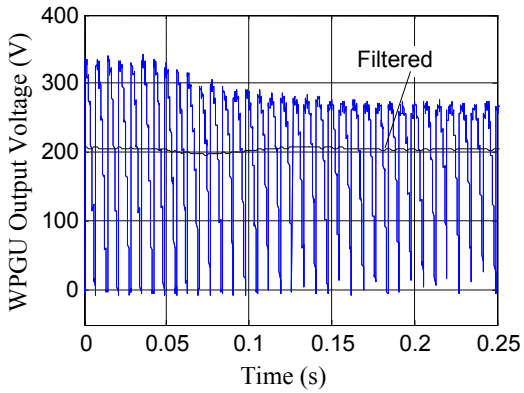

Fig. 11. The WPGU output voltage when the load impedance is decreased down from 175Ω to 58.5Ω, obtained experimentally.

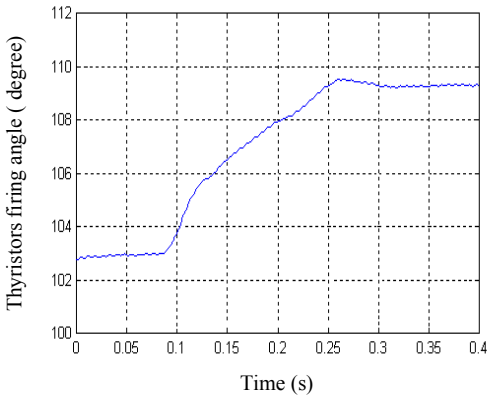

Fig. 12. The WPGU output voltage when the load impedance is increased from 35.5 Ω up to 88.5Ω.

This fact is plainly represented on the Figure 11, where the measured voltage at the output of the WPGU is shown along with its filtered curve. A 2nd-order Butterworth lowpass filter was used to obtain the filtered curve. A reference voltage of 200V was used.

Obviously, the DC output voltage produced by the WPGU remains constant even though the AC output voltage of the SEIG is greatly affected by the variation of load impedance.

The PI regulator ensures this voltage regulation by changing the firing angle of the thyristors, as shown on the Figure 12.

5 Conclusion

In this article, the wind power generating unit of an hybrid Photovoltaic – Wind renewable energy system (HPVWRES) was presented. The WPGU studied is equipped with a self-excited induction generator. A controlled AC/DC converter connected to the SEIG stator terminal provides a constant DC

voltage. The dynamic flux model of the self-excited induction generator used for the test was developed. The phenomenon of the magnetic saturation, indispensable for the operation of the SEIG, was particularly discussed and accounted for in the developed model. Experimental and computed results that describe the transients of the voltage buildup process as well as the transients of the connection of the load onto the SEIG stator terminals were presented. The comparison of all these results shows a very good agreement between the experimentation and simulation and thus confirms the validity of the developed model.

It was shown that the SEIG has a poor output characteristic. Indeed, the output voltage of the SEIG is highly influenced by the impedance of the load and the rotor speed. The use of the controlled AC/DC converter remedies to this drawback of the SEIG and gives a constant DC voltage for a large variation of the load and the rotor speed.

Experimental tests using a laboratory prototype of a three-phase semi-bridge converter were done. The experimental results presented in the previous section show the actual waveforms of the voltages at the output of both the SEIG and the whole WPGU. These results illustrate obviously the ability of the WPGU to produce a constant DC voltage for large disturbances that might be provoked by the variations of the load impedance and/or the rotor speed.

Acknowledgment:
The authors wish to thank for CMEP (project No. 03 MDU 592) for their support.

References:

[1] T. Senjyu, T. Nakaji, K. Uezato, T. Funabashi, A hybrid power system using alternative energy facilities in isolated island**,** *IEEE Trans. on Energy Conversion,* Vol.20, No.2, 2005, pp. 406-414.

[2] T.J. Hammons, J.C Boyer, S.R. Conners, M. Davies, M. Ellis, M. Fraser, E.A. Holt, J. Markard, Renewable energy alternatives for developed countries**,** *IEEE Trans. on Energy Conversion*, Vol.15, No.4, 2000, pp. 481 – 493.

[3] F. Blaabjerg, Zhe Chen, S.B. Kjaer, Power electronics as efficient interface in dispersed power generation systems**,** *IEEE Trans. on Power Electronics*, Vol.19, No.5, 2004, pp. 1184 – 1194.

[4] T. Ahmed, O. Noro, E. Hiraki, M. Nakaoka, Terminal voltage regulation characteristics by static var compensator for a three-phase self-excited induction generator, *IEEE Trans. on Industry Applications*, Vol.40, No.4, 2004, pp. 978 – 988.

[5] S.A. Daniel, N. Ammasai Gounden, A novel hybrid isolated generating system based on PV fed inverter-assisted wind-driven induction Generators, *Trans. on Energy Conversion*, Vo.19, No.2, 2004, pp. 416 – 422.

[6] F.A. Farret, B. Palle, M.G. Simoes, Full expandable model of parallel self-excited induction generators, *IEE Proceedings on Electric Power Applications*, Vol.152, No.1, 2005, pp. 96 – 102.

[7] B. Palle, M.G. Simoes, F.A. Farret, Dynamic Simulation and Analysis of Parallel Self-Excited Induction Generators for Islanded Wind Farm Systems, *IEEE Trans. on Industry Applications*, Vol.41, No.4, 2005, pp. 1099 – 1106.

[8] W.D. Kellogg, M.H. Nehrir, G. Venkataramanan, V. Gerez, Generation unit sizing and cost analysis for stand-alone wind, photovoltaic, and hybrid wind/PV systems, *IEEE Trans. on Energy Conversion*, Vol.13, No.1, 1998, pp. 70 – 75.

[9] E. D. Basset and F.M. Potter, Capacitive Excitation of Induction Generators, *Trans. Amer. Inst. Electr. Eng.*, 54, 1935, pp. 540-545.

[10] R. Ibtiouen A. Nesba S. Mekhtoub O. Touhami, An approach for the modeling of saturated induction machine, *Proc. International AEGAN Conference on Electrical Machines and Power Electronics, ACEMP'01,* Kasudasi-Turkey, 27-29 June, 2001, pp. 269-274.

[11] R. Ibtiouen, M. Benhaddadi, A. Nesba, S. Mekhtoub, O. Touhami, Dynamic performances of a self-excited induction generator feeding different static loads, *International Conference on Electrical Machines, Bruges, Belgium*,2002.

[12] P.C. Krause, *Analysis of electric machinery,* McGraw-Hill, 1987.